Amyloid-β induced membrane damage instigates tunnelling nanotubes and direct cell-to-cell transfer

Karin Ollinger[1], Katarina Kagedal[1] and Sangeeta Nath[2*]

[1]Experimental Pathology, Department of Clinical and Experimental Medicine, Linköping University, 581 85 Linköping, Sweden.

[2] Manipal Institute of Regenerative Medicine, Manipal Academy of Higher Education, Bangalore, 560065, India.

Abstract: The progressive pathology development in Alzheimer's disease is due to direct transfer of amyloid-β_{1-42} oligomers (oAβ) between connected neurons. However, the mechanism of transfer is not revealed yet. Here we show that internalization of toxic oAβ in SH-SY5Y cells, causes cellular stress detected as significant membrane surface expansion. Subsequently, protrusions appear in the form of tunnelling nanotubes (TNTs). The TNTs propagate oAβ and organelles directly from one cell-to-another. Preceding the formation, we detect oAβ induced plasma membrane damage and repair through lysosomal-exocytosis followed by endocytosis to re-establish the membrane. Eventually, the non-degradable internalized oligomers accumulate in lysosomes. Direct transfer of neurodegenerative proteins via TNTs has recently been suggested as means of pathology spreading. However, molecular basis of TNTs formation is unexplored. The present study is giving the insight that sprouting of TNTs might instigate as consequences of oAβ induced membrane damage and perturbed membrane repair process in the stressed cells, probably to maintain cell surface expansion and/or membrane-tension in equilibrium.

Summary: TNTs were recently discovered as novel route in cell-to-cell pathology spreading of many diseases. Here we show that TNTs instigate as a consequences of perturbed membrane repair process in oAβ accumulated stressed cells. The mechanistic understanding has enormous pathophysiology significance.

Short title: Direct cell-to-cell transfer of Aβ oligomers in TNTs.

Key words: Alzheimer's disease, Tunnelling nanotubes, amyloid-β, membrane repair, endocytosis-exocytosis, prion propagation.

*** Corresponding to be addressed to sangeeta.nath@manipal.edu**

Introduction. Neurodegenerative diseases are propagating disorders characterized by accumulation of misfolded proteins that form aggregates, plaque and eventually cause neurodegeneration. Prion like self-propagation and gradual pathology progression (Prusiner, 2013) in a predetermined pattern to different parts of the brain is a common hallmark of neurodegenerative diseases. Several studies have shown that proteins involved in these diseases such as tau, Aβ, α-synuclein and huntingtin follow common patterns including misfolding, self-propagation and neuron-to-neuron transfer (Clavaguera *et al.*, 2009; Desplats *et al.*, 2009; Ren *et al.*, 2009; Ilieva, Polymenidou and Cleveland, 2009; Hansen *et al.*, 2011). In a model of Alzheimer's disease (AD), we have previously shown that spreading of AD pathology is due to direct transfer of amyloidogenic oligomers of Aβ between connected neurons (Nath et al., 2012). Moreover, lysosomal stress due to gradual accumulation of toxic non-degradable oAβ enhances the progression and the cell-to-cell transfer correlates with insufficient lysosomal degradation. Interestingly, transfer happens much before the cells start to show detectable lysosomal toxicity (Domert et al., 2014). The studies (Nath et al., 2012; Domert et al., 2014) provided the possible explanations of how intracellular soluble oAβ reported as the potential initiator or driver of AD (Narasimhan *et al.*, 2017; Gouras *et al.*, 2010; Walsh and Selkoe, 2004), could develop gradual pathology by propagating between connected cells. However, mechanism of direct neuron-to-neuron propagation of neurodegenerative aggregates is not revealed yet.

Aβ induced neuronal dysfunction and impaired synaptic plasticity accountable for memory impairment reported to be propagated to the neighbouring cells (Kane *et al.*, 2000; Meyer-Luehmann *et al.*, 2006; Wei *et al.*, 2010), however studies did not reveal if such pathology propagation is due to direct trans-synaptic transfer of toxic Aβ. In addition, exosomes are investigated as means of cell-to-cell transfer of Aβ (Rajendran *et al.*, 2006; Sardar Sinha *et al.*, 2018). However, these studies could not explain the anatomically connected strict spatiotemporal pathology progression of AD. On the other hand, cell-to-cell transfers of both extracellular and intracellular monomers and protofibrils of $A\beta_{1-42}$ via TNTs are demonstrated

in the primary cultures of neurons and astrocytes (Wang et al., 2011). Recently, many studies demonstrated TNTs to transfer neurodegenerative proteins, such as PrP^{Sc}, α-synuclein, Aβ, tau, polyQ (Gousset *et al.*, 2009; Wang *et al.*, 2011; Zhu *et al.*, 2015; Tardivel *et al.*, 2016; Dieriks *et al.*, 2017), directly from one cell-to-another. Several of these studies implicated links between tunnelling nanotubes and endo-lysosomal pathway in cell-to-cell spreading (Bhat et al., 2018; Victoria and Zurzolo, 2017). These studies and the discovery of TNTs (Rustom et al., 2004) opened up new direction to prion like cell-to-cell propagation in neurodegenerative diseases. However, the molecular basis of TNTs formation is unexplored.

TNTs are open ended membrane nano-structures with membrane actin protrusions between neighbouring cells. The diameter of TNTs is reported to be between 50-200 nm (Gerdes et al., 2013). TNTs are transient structures, stay intact for minutes to hours. Membrane protrusions like filopodium precede TNT formation and inhibition of actin polymerization attenuates its formation (Bukoreshtliev et al., 2009). TNT formation prevails in neuronal cells and primary neurons (Rustom et al., 2004). Successive studies also showed TNT formation in different cell types, such as immune cells, fibroblast, epithelial cells, astrocytes and many others (Onfelt *et al.*, 2004; Davis and Sowinski, 2008; Gerdes and Carvalho, 2008).

In this study we show oAβ induced formation of TNTs between neighbouring SH-SY5Y cells and direct cell-to-cell propagation of oAβ and organelles. Internalization of toxic oligomers of oAβ, causes cellular stress detected as significant membrane surface expansion. Subsequently, TNTs protrude towards neighbouring cells. Preceding the formation of TNTs, we detect oAβ induced plasma membrane damage and repair through lysosomal exocytosis, and followed by coupled-endocytosis to re-establish the plasma membrane. Eventually, the internalized and transferred oligomers end up in lysosomes and non-degradable oligomers accumulates gradually. Altogether, observations are giving insights that the mechanism of TNT formation could be the consequences of perturbed membrane repair process in stressed cells. The study is also revealing the involvement of oAβ induced TNTs in direct neuron-to-neuron transfer of amyloid pathology in AD progression.

Results.

oAβ induce cellular stress and formation of TNTs.

Cell-to-cell propagation of Aβ aggregates has enormous implication in Alzheimer's disease for understanding the gradual progression of the pathology through anatomically connected brain

regions. Although cell-to-cell propagation of oAβ between connected cells have been shown in earlier studies (Wang *et al.*, 2011; Nath *et al.*, 2012; Domert *et al.*, 2014; Sardar Sinha *et al.*, 2018), however the mechanism is still unexplored. Here, we image the uptake of Aβ in differentiated SH-SY5Y cells, after washing and staining with LysoTracker (green). We observe that extracellularly applied oAβ-TMR (10 nM to 1 μM verified) get internalized efficiently and significant amount is found to end up in lysosomes within 30 min. We have quantified the internalization of 250 nM of oAβ-TMR (red) after 3 h of incubation and observed that 76 ± 14 % end up in lysosomes labelled with 200 nM of lysoTracker (green) by analysing co-localization percentage (Figure 1A). Morphologically these cells exhibit blebs and noticeable cell membrane expansion as well as nanotubes between neighbouring cells. Here, we show images of cells incubated for 3 h with 250 and 500 nM of oAβ-TMR (Supplementary Movie 1, Figure 1B). Moreover, we show that oligomers of Aβ travel unidirectional from one cell to another via TNTs (Figure 1B). The lengths of the TNTs are found to be between 0.2-16 μm. We did not observe TNT structures and unusual membrane expansions in the differentiated control cells (Figure 1C). Differentiated cells form neurites and in our previous studies we have extensively characterized neuronal properties of those cells (Agholme *et al.*, 2010; Nath *et al.*, 2012). In the neurites, organelles and lysoTracker positive lysosomes move anterograde-retrograde bi-directional (Supplementary Movie 2). We quantified the number of cells with unusual blebs / lamellipodia and TNTs with respect to the total number of cells and found concentration dependent increase, when quantifying at 200-500 nM of oAβ-TMR treated cells compare to the control cells (Figure 1D, E).

oAβ propagation to healthy cells is mediated by transport in TNTs.

To study how cells with accumulated Aβ transfer the material to neighbouring healthy cells, we have used a 3D donor-acceptor co-culture model that we earlier have designed (Nath *et al.*, 2012; Domert *et al.*, 2014). As acceptor cells, differentiated SH-SY5Y cells transfected with EGFP-tagged endosomal protein (green, Rab5a) were used, while the donor cells were incubated with oAβ-TMR (red). Co-cultures were prepared by seeding donor and acceptor cells in ECM gel on chambered glass slides and monitored in a confocal microscope. The images captured by time laps recording show transfer of oAβ-TMR donor (red) to acceptor cells (green) (Figure 2A). Interestingly, acceptor cell that had internalized oAβ-TMR forms TNTs towards healthy differentiated acceptor cell. Thus, the oAβ-TMR accumulated acceptor cells form transient filopodium like structures and blebs, which are not detected in matured differentiated neuronal controls. Noticeably, TNTs from stressed cells appear to grow from

bleb-like membrane protrusions (Figure 2A). Cells with blebs / lamellipodia and TNTs were quantified by counting the images of acceptor cells transferred with oligomers and donor cells. Acceptor cells having no transferred oAβ-TMR, appear healthy as judged by appearance of neurites and no significant blebs / lamellipodia (Figure 2B, C). DIC imaging using confocal microscope is not an ideal method for capturing of nano-scale TNTs structures, especially in a 3D co-culture cellular model. Thus, it is a risk of under estimation in quantification.

oAβ induce formation of TNTs independent of neuronal differentiation.

In order to clearly show that the studied TNTs structures are not neurites developed during neuronal cell differentiation, we performed the experiments in partially differentiated cells and undifferentiated SH-SY5Y neuronal cells. We have observed thin TNTs outspread from expanded lamellipodia-like membrane protrusions in partially differentiated SH-SY5Y cells internalized with oAβ-TMR after incubation with 250 nM of oligomers for 3 h. Furthermore, we detected unidirectional movement of oAβ-TMR colocalized with lysoTracker labelled lysosomes from one cell to another (Figure 3A). Similarly, we have observed TNTs outspread from expanded lamellipodia and unidirectional movements of organelles (Figure 3B). Moreover, the partially differentiated SH-SY5Y cells, form network of TNTs between neighbouring cells (Figure 3C, D; Supplementary Movie 3). The cells make network between 3 neighbouring cells via TNTs, and those TNTs were also outspread from expanded lamellipodia (Figure 3C). Formation of TNT networks between cells was also demonstrated in the prevailing article, where they showed TNTs as mode of intercellular cell communication (Rustom et al., 2004). We have also quantified oAβ-TMR induced cells with unusual blebs / lamellipodia and TNTs in partially differentiated cells treated with 250 nM of oAβ-TMR for 3 h (Figure 3F), compare to the control cells (Figure 3E).

We have extended the experiments with undifferentiated SH-SY5Y cells. As presented in Figure 4A, undifferentiated SH-SY5Y cells incubated with 1 μM of oligomeric Aβ together with the membrane dye TMA-DPH form TNTs within 10 min. Moreover, the oAβ induced TNT formation precedes the enhanced membrane activities, filopodium formation, blebs and massive endocytosis process as compared to the control cells (Figure 4 A-C; Supplementary Movie 4,5). oAβ induced massive endocytosis was quantified by measuring the internalized TMA-DPH from the luminal part of the cells (Figure 4C).

oAβ$_{1-42}$ induces membrane damage and lysosomal exocytosis.

oAβ induces TNT formation in association with the substantial enhancement of membrane activities and massive endocytosis, similarly as evident in Ca^{2+} dependent repair of injured plasma membrane (Idone et al., 2008), inspired us to determine if oAβ has a role in membrane damage. Previous reports have indicated that synthetic oAβ makes ion-permeable pores in synthetic membrane (Arispe, Pollard and Rojas, 1993; Kagan, 2012). A recent study has also shown that oligomers of Aβ can induce a membrane repair response (Julien *et al.*, 2018). Plasma membrane damage and influx of calcium has been shown to trigger lysosomal exocytosis and formation of a patch over the damage membrane to prevent cell lysis. Likewise, here we observe oAβ (1 μM) induced pore formation or membrane damage, detected as appearance of Lamp1 on the extracellular leaflet of the plasma membrane, in undifferentiated SH-SY5Y cells within 15-30 min of exposure (Figure 4E, F). To verify that the process is calcium dependent, we analysed influx of the membrane-impermeant dye propidium iodide (PI) in presence of 5 mM EGTA in PBS. The rationale behind this experiment is that if lysosomal exocytosis-dependent plasma membrane repair is occurring, chelation of Ca^{2+} will prevent the repair and PI will be detected intracellularly. As seen in Figure 4D, significant enhancement of PI staining was detected within 30 min after exposure to oAβ as quantified by flow cytometry and confocal imaging. Thus, we conclude that addition of 1 μM of oAβ, cause damage to the plasma membrane and as a membrane repair process lysosomal exocytosis and fusion of lysosomal membrane with the plasma membrane occur. Subsequent to the membrane repair process, re-establishment of the plasma membrane will occur by removing membrane parts through endocytosis and as a consequence oAβ internalizes into endosomes (Rab 5 positive structures) followed by entry into lysosomes (Lamp1 positive structures) (Figure 4G). Eventually the accumulation of non-degradable oAβ-TMR in lysosomes causes gradual development of extra-large lysosomes (Figure 3H). We have reported in our earlier study (Domert et al., 2014) that lysosomal stress develops by accumulated oligomers after 48 h.

Discussion. Prion like cell-to-cell propagation is a common characteristic of neurodegenerative diseases. Several reports have persistently reported direct cell-to-cell propagation of neurodegenerative protein aggregates and their implications in the gradual pathology progression (Clavaguera *et al.*, 2009; Desplats *et al.*, 2009; Ren *et al.*, 2009; Ilieva, Polymenidou and Cleveland, 2009; Hansen *et al.*, 2011). Our previous work has shown that, in AD gradual pathology progression is due to direct transfer of intracellularly accumulated non-

degradable soluble oAβ (Nath *et al.*, 2012; Domert *et al.*, 2014). However, the mechanism of cell-to-cell propagation is unexplored. Synaptic transfer has been investigated as a potential mechanism. Aβ induced spine loss and impaired synaptic plasticity are early pathologies and develop before neurodegeneration (Wei et al., 2010). Moreover, Aβ cause disruption of the synaptic transmission mediated by the synaptic receptors NMDA and AMPA (Walsh and Selkoe, 2004; Venkitaramani *et al.*, 2007). Therefore, neuron-to-neuron synaptic transmission of oAβ is unlikely. Likewise, inhibition of the possible receptors involved in synaptic transmission did not show any effect on the cell-to-cell transfer of Aβ in the cultured differentiated neuronal cells (Nath et al., 2012).

Aβ peptides are mainly generated extracellularly from transmembrane amyloid precursor protein (APP) by β- and γ-secretase enzymatic cleavage. Recent studies showed presence of β- and γ-secretase machineries and APP at the membranes of endo-lysosomes and generation of Aβ peptides in the lumen of endosomes and lysosomes (LaFerla, Green and Oddo, 2007; Gouras *et al.*, 2010; Edgar *et al.*, 2015). Increasingly the clinical studies and animal models indicate that soluble oAβ is the disease initiator and driver, rather than large extracellular depositions. Importantly, it was recently reported that the intracellular pool is mainly formed from aggregating prone and toxic Aβ42, while the less toxic Aβ40 is more abundant extracellularly (Sannerud et al., 2016). Intracellular accumulation of amyloidogenic proteins cause decreased lysosomal efficiency, detected as reduced degradation, abnormal lysosomal morphology and lysosomal membrane permeabilization as hallmark of neurodegenerative diseases (Freeman *et al.*, 2013; Eriksson *et al.*, 2017;Victoria and Zurzolo, 2017; Gowrishankar *et al.*, 2015). Lysosomes are central hubs for nutrient homeostasis but is also actively involved in cell death induction and plasma membrane repair. Stress signals from lysosomes also induce various signals affecting mitochondria, nucleus and dysregulates various cellular processes, and mediate increased oxidative stress (Appelqvist *et al.*, 2013; Ditaranto, Tekirian and Yang, 2001; Eriksson *et al.*, 2017; Freeman *et al.*, 2013). Several studies have indicated that ROS induced cellular stress enhances TNT formation (Rustom, 2016). Notably, lysosomal stress/damage due to accumulation of non-degradable amyloidogenic aggregates could induce formation of TNTs (Abounit et al., 2016) and cell-to-cell transfer of oAβ correlates with insufficient degradation efficiency of lysosomes (Domert et al., 2014).

In contrast, impaired processing of Aβ due to lysosomal enzymatic inefficiency and enhanced exocytosis was demonstrated by Annunziata *et al.*, 2013. Additionally, the study by Hase *et. al.* 2009 also reported that the exocyst complex involved in exosome fusion and membrane expansion regulates formation of TNTs. Plasma membrane recruitment of Ral-GTPase and

filamin, the actin remodeling proteins, also indicate positive regulating effects in TNT formation (Hase et al., 2009). The present study also demonstrates unusual membrane expansion, blebs, filopodium-like structures and outspread of TNTs from expanded membranes. Upregulation of exocyst complex during TNT formation might be prearrangement of rapid exocytosis as a Ca^{2+}dependent membrane repair process. The observation of active generation of Ca^{2+} and its propagation through TNTs has already been reported by Smith et al., 2011. Recently, it was also shown that oligomers of Aβ can induce a membrane repair response similar to that induced by exposure to the bacterial pore-forming toxin produced by *B. thuringensis* (Julien *et al.*, 2018). Consequently, enhanced internalization of Aβ occur via endocytosis, which is independent of receptor interactions.

Internalization of the oAβ pool appears to occur via early endosomes and is directed to lysosomes, where non-degradable aggregation prone oAβ gradually induce lysosomal stress. Notably, propagation of amyloidogenic seeds was observed much earlier, whereas lysosomal pathology develops gradually over time (Domert et al., 2014). Involvement of the endo-lysosomal pathway is also relevant in maintaining cellular homeostasis by regulating membrane stress and cell surface expansion (Apodaca, 2017; Thottacherry *et al.*, 2018). Exocytosis is involved in the expansion of cell surface area and results in decreased membrane stress. Simultaneously, the process of endocytosis follows to re-establish the membrane area or to re-establish the membrane stress. Recent studies have shown the formation of tubular-like filopodium structures, membrane invaginations/blebs during induction of reduced cellular stress (Norman *et al.*, 2010;Sinha *et al.*, 2011;Kosmalska *et al.*, 2015). Similarly, the TNTs form from protrusions in response to rapid membrane repair could be the consequences of perturbed membrane repair process in cells stress by accumulated oligomers, probably to maintain the membrane stress and cell surface expansion in equilibrium.

Several studies have suggested exosomes as means of cell-to-cell transfer of Aβ (Rajendran *et al.*, 2006; Sardar Sinha *et al.*, 2018). However, such experiments were designed at non-physiological conditions, with purified concentrated exosomes from large number of cultured cells. Additionally, a transfer mechanism via exosomes is unable to explain the asymmetric spreading of oAβ microinjected in a single neuron of primary hippocampal culture (Nath et al., 2012). Studies using the method of transwell assays have also shown the efficient transfer of prion proteins between cell-to-cell despite the blocking of exosomes (Gousset *et al.*, 2009; Thayanithy *et al.*, 2017). The studies indicated the possible mechanism of direct cell-to-cell transfer via TNTs. On the other hand, organelles like toxic lysosomes have been demonstrated to propagate directly cell-to-cell through TNTs (Victoria and Zurzolo, 2017). Moreover,

increasingly reports of cell-to-cell transfer of common neurodegenerative proteins via TNTs, such as PrP^{Sc}, α-synuclein, tau, polyQ aggregates and Aβ, instigate new avenues (Gousset *et al.*, 2009; Wang *et al.*, 2011; Zhu *et al.*, 2015; Tardivel *et al.*, 2016; Dieriks *et al.*, 2017). TNTs as means of direct neuron-to-neuron transfer is a convincing model of how the oligomers suggested as initiator or driver of AD pathology could gradually progress through the anatomically connected brain regions. The hypothesis is important in the context of progressive AD pathology development, as plaque pathology poorly correlates with progressive cognitive impairment in AD. Here, our study gives insight that the formation of TNTs could be the consequences of perturbed equilibrium balance between coupled endocytosis-exocytosis during rapid membrane repair (Figure 5). However, further in-depth studies are needed to understand how cells maintain homeostasis of intercellular communication by balancing exosome release and TNTs in the stressed cells. It is also important to unfold the involvement of cell surface expansion and endo-lysosomal pathway in the induction of TNTs formation at molecular level.

Unfolding of molecular basis of TNT formation is immensely demanding, as it is an important intercellular communication mechanism of stressed cells reported in many diseases like neurodegenerative diseases, HIV-1 infection (Sowinski et al., 2008; Hashimoto et al., 2016), Influenza virus (Kumar et al., 2017), Herpesvirus transmission (Panasiuk et al., 2018) and cancer (Lou et al., 2012). Recent, lattice light sheet imaging directly visualized membrane nanotubes *in situ*, in interconnecting breast cancer cells in live acute brain slices (Parker *et al.*, 2017). Thus, the understanding the mechanism of TNT formation has huge pathophysilogical significance. The study will open up a new avenue to unfold and explore an emerging novel pathway of intercellular cell-to-cell communication.

Material and Methods.

Preparation of soluble oAβ. Freshly made unlabelled oAβ and fluorescently labelled oAβ-TMR were prepared from lyophilized Aβ ($Aβ_{1–42}$) and Aβ-TMR ($Aβ_{1–42}$-5-tetramethyl rhodamin) suspended in 1,1,1,3,3,3-hexafluoro-2-propanol (AnaSpec). Lyophilized Aβ and Aβ-TMR were resuspended at a concentration of 5 mM in Me2SO and then diluted to a concentration of 100 μM in HEPES buffer, pH 7.4. The solution was immediately vortexed and sonicated for 2 min and then incubated at 4°C for 24 h (Catalano et al., 2006; Nath et al; Domert et al). Oligomers were characterized before doing the experiments similarly as reported

in our earlier papers (Nath *et al.*, 2012; Domert *et al.*, 2014), by electron microscopy imaging using Jeol 1230 transmission electron microscope equipped with an ORIUS SC 1000 CCD camera, together with SDS-PAGE, Native-PAGE western blots and size exclusion chromatography.

Cell culture and differentiation of cells. SH-SY5Y neuronal cells (ECACC; Sigma-Aldrich) were seeded on 10-mm glass-bottom Petri dishes (MatTek) at a concentration of 12,000 cells/cm^2. Cells were partially differentiated with 10 μM retinoic acid (RA; Sigma-Aldrich) for 7 days. Pre-differentiated or partially differentiated SH-SY5Y cells were further differentiated for additional 10 days in 10-mm glass-bottom Petri dishes (MatTek) with brain-derived neurotrophic factor, neuregulin-1, nerve growth factor, and vitamin D3. After 10 days of differentiation on glass, the cells form long, branched neurites and several neurospecific markers, as described previously (Agholme *et al.*, 2010; Nath *et al.*, 2012). Partially differentiated and differentiated cells on glass petri dishes were incubated with 100–500 nM oAβ–TMR for 3 h at 37°C in a 5% CO_2 atmosphere. The cells were imaged after extensive PBS washing (two washes of 10 min each at 37°C with 5% CO_2). LysoTracker (green; Invitrogen) 50-250 nM were added 5-10 min before imaging.

Donor-acceptor 3D co-culture. Three dimensional donor-acceptor co-culturing was performed using RA treated partially differentiated cells for 10 days in ECM gel (1:1; Sigma-Aldrich), as described earlier (Nath *et al.*, 2012; Domert *et al.*, 2014). The differentiated cells in ECM gel have been well characterized previously; they had long, branched neurites, several neurospecific markers, synapse protein Sv2, axonal vesicle transport and mature splicing forms of tau (Agholme *et al.*, 2010; Nath *et al.*, 2012). The differentiated cells were stained green with EGFP-tagged (green) endosomal (Rab5a) or lysosomal (Lamp1) proteins using organelle lights BacMam-1.0 or 2.0 (Invitrogen). The green labelled differentiated cells were called ‘acceptor cells’. Pre-differentiated cells (10 μM RA for 7 days in 35-mm cell-culture Petri dishes) incubated with 500 nM oAβ-TMR for 3 h at 37°C in a 5% CO_2 atmosphere; extensively washed using PBS (two washes of 10 min each at 37°C with 5% CO_2) and trypsinized, were denoted as ‘donor cells’ reseeded (40,000 cells per dish) on top of the acceptor cells after mixing (1:1) with prechilled ECM gel. Then, the 3D donor-acceptor co-cultured cells were incubated for 24 h with 10 μM RA at 37°C in a 5% CO_2 atmosphere.

Immunocytochemistry. Lamp1 staining on the luminal part of the plasma membrane in undifferentiated SH-SY5Y neuroblastoma cells was performed similarly as described earlier (Wäster et al., 2016), on unfixed cells. Cells were incubated for 15 and 30 min with 1 µM of oAβ in MEM media without FCS (fetal calf serum) supplement. Then endocytosis of the cells were blocked with 5% BSA + 10% FCS in PBS for 5 min at 4 °C. Then cells were incubated with Lamp1-anti goat primary antibody (1:250, sc-8099, Santa Cruz Bio-technology; Santa Cruz, CA, USA; 2 h, 4 °C) in the blocking buffer for 45 min, ffollowed by fixation of the cells in 4% PFA for 20 min at 4 °C before labelling with the secondary antigoat antibody conjugated to Alexa Fluor 488 (1:400 for 30 min; Molecular Probes, Eugene, OR, USA). Next, the cells were mounted in ProLong Gold antifade reagent supplemented with 4′,6-diamidino-2-phenylindole (DAPI; Molecular Probes).

Propidium Iodide staining: Undifferentiated SH-SY5Y cells were incubated with 1 µM of oAβ for 15 or 30 min at 37 °C. Then the cells were washed and stained with propidium iodide (PI, 5 µg/ml) by incubating for 5 min. Cells were washed again two times with PBS before applying 4 % PFA as fixative for 20 min at 4 °C. The fixed cells were observed by confocal microscopy or trypsinized before analyzing by flow cytometer.

Live cell imaging of membrane dynamics: oAβ of concentration 1 µM was added concurrently with 0.5 µM of membrane binding dye TMA-DPH (N,N,N-Trimethyl-4-(6-phenyl-1,3,5-hexatrien-1-yl) phenylammonium p-toluenesulfonate; molecular formula: $C_{28}H_{31}NO_3S$) and membrane dynamics of the live cells were followed by timelaps images using a confocal microscope. The excitation and emission maximum of TMA-DPH is 384 and 430 nm, with considerable tail of excitation spectra at 405 nm. Therefore, time-lapse images were taken using confocal-microscope by exciting the TMA-DPH dye using the 405 nm laser and sufficient emission light was collected using an opened pinhole. In this setup confocal microscope produces images similar to the widefield or epifluorescence images. Cultures were carried to the microscope one by one in 500 µl of 20 mM Hepes buffer of pH 7.4 maintaining the temperature at 37 ° C.

Confocal microscopy and flow-cytometry. All images were acquired using a Zeiss LSM laser scanning confocal microscope using 63x/1.40 NA or 40X/1.3 NA oil immersion plan-apochromatic objective (Carl Zeiss AG, Oberkochen, Germany). The time-laps image sequences of the live cells were taken at 37 °C by capturing simultaneously differential

interference contrast (DIC) and fluorescence modes. Cells internalized with propidium iodide (PI) were fixed, trypsinized and filtered using CellTrics 30 μm filters (Sysmex). Then re-suspended in PBS and quantified using BD FACS Aria ™ (BD Biosciences) flow cytometer.

Image analysis. Image analysis were done by ImageJ software (open source by NIH, USA). Percentage of co-localization of oAβ (red) with lysosomes (green) were performed by calculating the proportion of the red fluorescence pixels compared to the co-localized pixels from background subtracted images using Coloc-2 plugin. Cells with blebs / lamillopodia and TNTs were counted from images and normalized with total number of cells. oAβ induced endocytosis was quantified by measuring the integrated intensities of internalized TMA-DPH from the luminal part of each cells by drawing ROI (region of interest) over sequences of time-laps confocal image stacks and compared the same quantification with control cells. The fusion of lysosomal membrane to reseal the membrane damaged was detected as appearance of LAMP1 (green) on the outer leaflet of the plasma membrane. The outer leaflet LAMP1 was quantified measuring the integrated intensities from drawn ROI and proportionate percentage calculated comparing the total LAMP1 per cells.

Acknowledgement: This research was made possible by funding from the Swedish Alzheimer's Foundation, Magnus Bergvalls and Gun och Bertil Stohnes research grants from Sweden and Research Assistant Professor intramural grants of Manipal Academy of Higher Education, India. We thank our long-term collaborator Prof. Martin Hallbeck of Linkoping University, Sweden, for the valuable suggestions on designing of cell-to-cell transfer experiments. We thank Prof. Satyajit Mayor of National centre for biological sciences, India, and Prof. Gopal Pande of Manipal institute of higher education, India, for reading the manuscript and for their valuable inputs.

Author Contributions: : S.N conceptualized and conducted the research; S.N and K.O designed research; S.N designed tunnelling nanotube experiments; K.O. designed membrane dynamics and membrane repair experiments; S.N performed experiments; S.N, K.O and K.K interpreted data; S.N wrote the paper taking valuable inputs from K.O and K.K.

Abbreviations.

AD - Alzheimer's disease.

oAβ - Oligomers of amyloid-β (1-42)

oAβ-TMR – Tetramethyl rhodamin labelled oligomers of amyloid-β (1-42)

TNTs- Tunnelling nanotubes

LAMP-1 - Lysosomal associated membrane protein-1

References.

Abounit, S., J.W. Wu, K. Duff, G.S. Victoria, and C. Zurzolo. 2016. Tunneling nanotubes: A possible highway in the spreading of tau and other prion-like proteins in neurodegenerative diseases. *Prion.* 10:344–351.

Agholme, L., T. Lindström, K. Kgedal, J. Marcusson, and M. Hallbeck. 2010. An in vitro model for neuroscience: Differentiation of SH-SY5Y cells into cells with morphological and biochemical characteristics of mature neurons. *J. Alzheimer's Dis.* 20:1069–1082.

Annunziata, I., A. Patterson, D. Helton, H. Hu, S. Moshiach, E. Gomero, R. Nixon, and A. D'Azzo. 2013. Lysosomal NEU1 deficiency affects amyloid precursor protein levels and amyloid-β secretion via deregulated lysosomal exocytosis. *Nat. Commun.* 4.

Apodaca, G. 2002. Modulation of membrane traffic by mechanical stimuli. *Am. J. Physiol. Renal Physiol.* 282:F179-90.

Appelqvist, H., P. Wäster, K. Kågedal, and K. Öllinger. 2013. The lysosome: From waste bag to potential therapeutic target. *J. Mol. Cell Biol.* 5:214–226.

Arispe, N., H.B. Pollard, and E. Rojas. 1993. Giant multilevel cation channels formed by Alzheimer disease amyloid beta-protein [A beta P-(1-40)] in bilayer membranes. *Proc. Natl. Acad. Sci. U. S. A.* 90:10573–7.

Bhat, S., C. Zurzolo, S. Zhu, S. Syan, Y. Kuchitsu, and M. Fukuda. 2018. Rab11a–Rab8a cascade regulates the formation of tunneling nanotubes through vesicle recycling. *J. Cell Sci.*

Bukoreshtliev, N. V., X. Wang, E. Hodneland, S. Gurke, J.F.V. Barroso, and H.H. Gerdes. 2009. Selective block of tunneling nanotube (TNT) formation inhibits intercellular organelle transfer between PC12 cells. *FEBS Lett.* 583:1481–1488.

Clavaguera, F., T. Bolmont, R.A. Crowther, D. Abramowski, S. Frank, A. Probst, G. Fraser, A.K. Stalder, M. Beibel, M. Staufenbiel, M. Jucker, M. Goedert, and M. Tolnay. 2009. Transmission and spreading of tauopathy in transgenic mouse brain. *Nat. Cell Biol.* 11:909–913.

Davis, D.M., and S. Sowinski. 2008. Membrane nanotubes: Dynamic long-distance connections between animal cells. *Nat. Rev. Mol. Cell Biol.* 9:431–436.

Desplats, P., H.-J. Lee, E.-J. Bae, C. Patrick, E. Rockenstein, L. Crews, B. Spencer, E. Masliah, and S.-J. Lee. 2009. Inclusion formation and neuronal cell death through neuron-to-neuron transmission of -synuclein. *Proc. Natl. Acad. Sci.* 106:13010–13015.

Dieriks, B.V., T.I.H. Park, C. Fourie, R.L.M. Faull, M. Dragunow, and M.A. Curtis. 2017. α-synuclein transfer through tunneling nanotubes occurs in SH-SY5Y cells and primary brain pericytes from Parkinson's disease patients. *Sci. Rep.* 7.

Ditaranto, K., T.L. Tekirian, and A.J. Yang. 2001. Lysosomal membrane damage in soluble Aβ-mediated cell death in Alzheimer's disease. *Neurobiol. Dis.* 8:19–31.

Domert, J., S.B. Rao, L. Agholme, A.C. Brorsson, J. Marcusson, M. Hallbeck, and S. Nath. 2014. Spreading of amyloid-β peptides via neuritic cell-to-cell transfer is dependent on insufficient cellular clearance. *Neurobiol. Dis.* 65:82–92.

Edgar, J.R., K. Willén, G.K. Gouras, and C.E. Futter. 2015. ESCRTs regulate amyloid precursor protein sorting in multivesicular bodies and intracellular amyloid-β accumulation. *J. Cell Sci.* 128:2520–2528.

Eriksson, I., S. Nath, P. Bornefall, A.M.V. Giraldo, and K. Öllinger. 2017. Impact of high cholesterol in a Parkinson's disease model: Prevention of lysosomal leakage versus stimulation of α-synuclein aggregation. *Eur. J. Cell Biol.* 96:99–109.

Freeman, D., R. Cedillos, S. Choyke, Z. Lukic, K. McGuire, S. Marvin, A.M. Burrage, S. Sudholt, A. Rana, C. O'Connor, C.M. Wiethoff, and E.M. Campbell. 2013. Alpha-Synuclein Induces Lysosomal Rupture and Cathepsin Dependent Reactive Oxygen Species Following Endocytosis. *PLoS One*. 8.

Gerdes, H.H., and R.N. Carvalho. 2008. Intercellular transfer mediated by tunneling nanotubes. *Curr. Opin. Cell Biol.* 20:470–475.

Gerdes, H.H., A. Rustom, and X. Wang. 2013. Tunneling nanotubes, an emerging intercellular communication route in development. *Mech. Dev.* 130:381–387.

Gouras, G.K., D. Tampellini, R.H. Takahashi, and E. Capetillo-Zarate. 2010. Intraneuronal β-amyloid accumulation and synapse pathology in Alzheimer's disease. *Acta Neuropathol.* 119:523–541.

Gousset, K., E. Schiff, C. Langevin, Z. Marijanovic, A. Caputo, D.T. Browman, N. Chenouard, F. de Chaumont, A. Martino, J. Enninga, J.C. Olivo-Marin, D. Männel, and C. Zurzolo. 2009. Prions hijack tunnelling nanotubes for intercellular spread. *Nat. Cell Biol.* 11:328–336.

Gowrishankar, S., P. Yuan, Y. Wu, M. Schrag, S. Paradise, J. Grutzendler, P. De Camilli, and S.M. Ferguson. 2015. Massive accumulation of luminal protease-deficient axonal lysosomes at Alzheimer's disease amyloid plaques. *Proc. Natl. Acad. Sci.* 112:E3699–E3708.

Hase, K., S. Kimura, H. Takatsu, M. Ohmae, S. Kawano, H. Kitamura, M. Ito, H. Watarai, C.C. Hazelett, C. Yeaman, and H. Ohno. 2009. M-Sec promotes membrane nanotube formation by interacting with Ral and the exocyst complex. *Nat. Cell Biol.* 11:1427–1432.

Hashimoto, M., F. Bhuyan, M. Hiyoshi, O. Noyori, H. Nasser, M. Miyazaki, T. Saito, Y. Kondoh, H. Osada, S. Kimura, K. Hase, H. Ohno, and S. Suzu. 2016. Potential Role of the Formation of Tunneling Nanotubes in HIV-1 Spread in Macrophages. *J. Immunol.* 196:1832–1841.

Idone, V., C. Tam, J.W. Goss, D. Toomre, M. Pypaert, and N.W. Andrews. 2008. Repair of injured plasma membrane by rapid Ca2+ dependent endocytosis. *J. Cell Biol.* 180:905–914.

Ilieva, H., M. Polymenidou, and D.W. Cleveland. 2009. Non-cell autonomous toxicity in neurodegenerative disorders: ALS and beyond. *J. Cell Biol.* 187:761–772.

Julien, C., C. Tomberlin, C.M. Roberts, A. Akram, G.H. Stein, M.A. Silverman, and C.D. Link. 2018. In vivo induction of membrane damage by β-amyloid peptide oligomers. *Acta Neuropathol. Commun.* 6:131.

Kagan, B.L. 2012. Membrane pores in the pathogenesis of neurodegenerative disease. *Prog. Mol. Biol. Transl. Sci.* 107:295–325.

Kane, M.D., W.J. Lipinski, M.J. Callahan, F. Bian, R.A. Durham, R.D. Schwarz, A.E. Roher, and L.C. Walker. 2000. Evidence for seeding of beta -amyloid by intracerebral infusion of Alzheimer brain extracts in beta -amyloid precursor protein-transgenic mice. *J. Neurosci.* 20:3606–11.

Kosmalska, A.J., L. Casares, A. Elosegui-Artola, J.J. Thottacherry, R. Moreno-Vicente, V. González-Tarragó, M.Á. Del Pozo, S. Mayor, M. Arroyo, D. Navajas, X. Trepat, N.C. Gauthier, and P. Roca-Cusachs. 2015. Physical principles of membrane remodelling during cell mechanoadaptation. *Nat. Commun.* 6.

Kumar, A., J.H. Kim, P. Ranjan, M.G. Metcalfe, W. Cao, M. Mishina, S. Gangappa, Z. Guo, E.S. Boyden, S. Zaki, I. York, A. García-Sastre, M. Shaw, and S. Sambhara. 2017. Influenza virus exploits tunneling nanotubes for cell-to-cell spread. *Sci. Rep.* 7.

LaFerla, F.M., K.N. Green, and S. Oddo. 2007. Intracellular amyloid-beta in Alzheimer's disease. *Nat. Rev. Neurosci.* 8:499–509.

Lou, E., S. Fujisawa, A. Morozov, A. Barlas, Y. Romin, Y. Dogan, S. Gholami, A.L. Moreira, K. Manova-Todorova, and M.A.S. Moore. 2012. Tunneling nanotubes provide a unique conduit for intercellular transfer of cellular contents in human malignant pleural mesothelioma. *PLoS One*. 7.

Melki, R., J.-Y. Li, E. Angot, C. Hansen, P. Brundin, J.A. Steiner, T.F. Outeiro, A.-L. Bergström, P. Kallunki, G. Paul, K. Fog, and L. Pieri. 2011. α-Synuclein propagates from mouse brain to grafted dopaminergic neurons and seeds aggregation in cultured human cells. *J. Clin. Invest.* 121:715–725.

Meyer-Luehmann, M., J. Coomaraswamy, T. Bolmont, S. Kaeser, C. Schaefer, E. Kilger, A. Neuenschwander, D. Abramowski, P. Frey, A.L. Jaton, J.M. Vigouret, P. Paganetti, D.M. Walsh, P.M. Mathews, J. Ghiso, M. Staufenbiel, L.C. Walker, and M. Jucker. 2006. Exogenous induction of cerebral β-amyloidogenesis is governed bf agent and host. *Science (80-.).* 313:1781–1784.

Narasimhan, S., J.L. Guo, L. Changolkar, A. Stieber, J.D. McBride, L. V. Silva, Z. He, B. Zhang, R.J. Gathagan, J.Q. Trojanowski, and V.M.Y. Lee. 2017. Pathological Tau Strains from Human Brains Recapitulate the Diversity of Tauopathies in Nontransgenic Mouse Brain. *J. Neurosci.* 37:11406–11423.

Nath, S., L. Agholme, F.R. Kurudenkandy, B. Granseth, J. Marcusson, and M. Hallbeck. 2012. Spreading of Neurodegenerative Pathology via Neuron-to-Neuron Transmission of -Amyloid. *J. Neurosci.* 32:8767–8777.

Norman, L.L., J. Bruges, K. Sengupta, P. Sens, and H. Aranda-Espinoza. 2010. Cell blebbing and membrane area homeostasis in spreading and retracting cells. *Biophys. J.* 99:1726–1733.

Onfelt, B., S. Nedvetzki, K. Yanagi, and D.M. Davis. 2004. Cutting edge: Membrane nanotubes connect immune cells. *J. Immunol.* 173:1511–3.

Panasiuk, M., M. Rychłowski, N. Derewońko, and K. Bieńkowska-Szewczyk. 2018. Tunneling Nanotubes as a Novel Route of Cell-to-Cell Spread of Herpesviruses. *J. Virol.* 92.

Prusiner, S.B. 2013. Biology and Genetics of Prions Causing Neurodegeneration. *Annu. Rev. Genet.* 47:601–623.

Rajendran, L., M. Honsho, T.R. Zahn, P. Keller, K.D. Geiger, P. Verkade, and K. Simons. 2006. Alzheimer's disease beta-amyloid peptides are released in association with exosomes. *Proc. Natl. Acad. Sci.* 103:11172–11177.

Ren, P.H., J.E. Lauckner, I. Kachirskaia, J.E. Heuser, R. Melki, and R.R. Kopito. 2009. Cytoplasmic penetration and persistent infection of mammalian cells by polyglutamine aggregates. *Nat. Cell Biol.* 11:219–225.

Rustom, A. 2016. The missing link: Does tunnelling nanotube-based supercellularity provide a new understanding of chronic and lifestyle diseases? *Open Biol.* 6.

Rustom, A., R. Saffrich, I. Markovic, P. Walther, and H.H. Gerdes. 2004. Nanotubular Highways for Intercellular Organelle Transport. *Science (80-.).* 303:1007–1010.

Sannerud, R., C. Esselens, P. Ejsmont, R. Mattera, L. Rochin, A.K. Tharkeshwar, G. De Baets, V. De Wever, R. Habets, V. Baert, W. Vermeire, C. Michiels, A.J. Groot, R. Wouters, K. Dillen, K. Vints, P. Baatsen, S. Munck, R. Derua, E. Waelkens, G.S. Basi, M. Mercken, M. Vooijs, M. Bollen, J. Schymkowitz, F. Rousseau, J.S. Bonifacino, G. Van Niel, B. De Strooper, and W. Annaert. 2016. Restricted Location of PSEN2/γ-Secretase Determines Substrate Specificity and Generates an Intracellular Aβ Pool. *Cell*. 166:193–208.

Sardar Sinha, M., A. Ansell-Schultz, L. Civitelli, C. Hildesjö, M. Larsson, L. Lannfelt, M. Ingelsson, and M. Hallbeck. 2018. Alzheimer's disease pathology propagation by exosomes containing toxic amyloid-beta oligomers. *Acta Neuropathol.* 136:41–56.

Sinha, B., D. Köster, R. Ruez, P. Gonnord, M. Bastiani, D. Abankwa, R. V. Stan, G. Butler-Browne, B. Vedie, L. Johannes, N. Morone, R.G. Parton, G. Raposo, P. Sens, C. Lamaze, and P. Nassoy. 2011. Cells respond to mechanical stress by rapid disassembly of caveolae. *Cell*. 144:402–413.

Smith, I.F., J. Shuai, and I. Parker. 2011. Active generation and propagation of Ca2+ signals within tunneling membrane nanotubes. *Biophys. J.* 100.

Tardivel, M., S. Bégard, L. Bousset, S. Dujardin, A. Coens, R. Melki, L. Buée, and M. Colin. 2016. Tunneling nanotube (TNT)-mediated neuron-to neuron transfer of pathological Tau protein assemblies. *Acta Neuropathol. Commun.* 4:117.

Thayanithy, V., P. O'Hare, P. Wong, X. Zhao, C.J. Steer, S. Subramanian, and E. Lou. 2017. A transwell assay that excludes exosomes for assessment of tunneling nanotube-mediated intercellular communication. *Cell Commun. Signal.* 15:1–16.

Thottacherry, J.J., A.J. Kosmalska, A. Kumar, A.S. Vishen, A. Elosegui-Artola, S. Pradhan, S. Sharma, P.P. Singh, M.C. Guadamillas, N. Chaudhary, R. Vishwakarma, X. Trepat, M.A. del Pozo, R.G. Parton, M. Rao, P. Pullarkat, P. Roca-Cusachs, and S. Mayor. 2018. Mechanochemical feedback control of dynamin independent endocytosis modulates membrane tension in adherent cells. *Nat. Commun.* 9.

Venkitaramani, D. V., J. Chin, W.J. Netzer, G.K. Gouras, S. Lesne, R. Malinow, and P.J. Lombroso. 2007. -Amyloid Modulation of Synaptic Transmission and Plasticity. *J. Neurosci.* 27:11832–11837.

Victoria, G.S., and C. Zurzolo. 2017. The spread of prion-like proteins by lysosomes and tunneling nanotubes: Implications for neurodegenerative diseases. *J. Cell Biol.* 216:2633–2644.

Walsh, D.M., and D.J. Selkoe. 2004. Deciphering the molecular basis of memory failure in Alzheimer's disease. *Neuron*. 44:181–93.

Wang, Y., J. Cui, X. Sun, and Y. Zhang. 2011. Tunneling-nanotube development in astrocytes depends on p53 activation. *Cell Death Differ.* 18:732–742.

Wäster, P., I. Eriksson, L. Vainikka, I. Rosdahl, and K. Öllinger. 2016. Extracellular vesicles are transferred from melanocytes to keratinocytes after UVA irradiation. *Sci. Rep.* 6.

Wei, W., L.N. Nguyen, H.W. Kessels, H. Hagiwara, S. Sisodia, and R. Malinow. 2010. Amyloid beta from axons and dendrites reduces local spine number and plasticity. *Nat. Neurosci.* 13:190–196.

Zhu, S., G.S. Victoria, L. Marzo, R. Ghosh, and C. Zurzolo. 2015. Prion aggregates transfer through tunneling nanotubes in endocytic vesicles. *Prion*. 9:125–135.

Figure Legends

Figure 1. A) Differentiated SH-SY5Y cells were incubated with 250 nM of oAβ-TMR (red) for 3 h, washed and imaged by labelling with LysoTracker (200 nM; green). oAβ-TMR ends up in lysosomes labelled with lysotracker. B) Connected nanotubes (highlighted by rectangle boxes) between neighbouring cells detected in differentiated SH-SY5Y cells incubated for 3 h with 500 nM of oAβ-TMR (red), washed and stained with 50 nM of lysotracker (green) before taking the image. The cells with long TNTs form noticeable blebs, filopodium and cell membrane expansion (indicated by black arrows). Unidirectional movements of oAβ-TMR were observed, indicated by white arrows in the sequence of images. C) Differentiated control cells show neuritic connections. The cells are also devoid of TNTs and unusual blebs or filopodium like structures. D) Percent of cells with blebs / lamellipodia were quantified from the images taken with increasing concentrations of oAβ-TMR (200-500 nM) and compared with the control cells. E) Similarly the number of TNTs were quantified with respect to the total number of cells. Quantifications were done from > 60 cells in each sets. Plots are mean ± SD. One-way ANOVA test were performed to validate statistical significance. Scale bars are 10 μm.

Figure 2. The 3D donor-acceptor cell model was desinged by donor cells allowed to accumulate oAβ-TMR (red) before co-cultured for 24 h with acceptor cells transfected with EGFP-tagged (green) Lamp1. A) TNT formed towards a healthy acceptor cell (marked 2) from the acceptor cell (marked 1) that already accumulated oAβ-TMR. Box 1 shows enlargement of transient filopodium (black arrows). Box 2 shows TNT formation from expanded membrane protrusions, bleb like structures (white arrow). B) Percent of cells with blebs / lamellipodia in oAβ-TMR accumulated donor and acceptor cells were quantified by counting images after 24 h of co-culture and compare with the healthy acceptor cells with no accumulation of oAβ-TMR. C) Number of TNTs were also quantified with respect to the total number of donor and acceptor cells, respectively. Quantifications were done from > 30 cells in each sets. Plots are mean ± SD. One-way ANOVA test were performed to validate statistical significance. Scale bar is10 μm.

642 **Figure 3.** Partially differentiated SH-SY5Y cells were incubated with 250 nM of oAβ-TMR
643 (red) for 3 h, washed and labelled with 200 nM of lysotracker (green). Cells internalized oAβ-
644 TMR and the oligomers accumulate to lysosomes. A) The cells form thin TNTs outspread from
645 expanded lamellipodia like membrane protrusions (black arrows). oAβ-TMR colocalized with
646 a lysosome moves unidirectional away from one cell to another (white arrows). B) TNTs
647 outspread from expanded lamellipodia-like membrane protrusions (black arrows) and
648 unidirectional movements of an organell (white arrows). C) Network between 3 neighbouring
649 cells via formation of TNTs (white arrows), outspread from lamellipodia-like membrane
650 protrusions (black arrows). D) TNTs form networks between two neighbouring cells (black
651 arrow) (Supplementary Movie 3). E) Partially differentiated control cells devoid of blebs /
652 lamellipodia. F) Percent of cells with blebs / lamellipodia in oAβ-TMR treated cells were
653 quantified and compared with the control cells. Number of TNTs were also quantified by
654 manually counting from cell images and plotted with respect to the total number of cells in
655 percentage. Plots are mean ± SD. Quantifications were done from > 60 cells in each sets. One-
656 way ANOVA test were performed to validate statistical significance. Scale bars are10 μm.
657
658
659 **Figure 4.** A) Undifferentiated SH-SY5Y cells incubated with 1 μM of oAβ together with the
660 membrane dye TMA-DPH (0.5 μM) and imaged immediately after addition. TNT formation
661 (white arrows) were observed (Box 1 and 2) within 10 min, preceding of massive membrane
662 activities, filopodium formation and endocytosis of membranes. B) Control cells show no
663 blebs, filopodium or TNT structures. C) Internalization or endocytosis of plasma membranes
664 labelled with TMA-DPH, were quantified in control and oAβ treated cells by measuring
665 luminal part of intensities over time. The plot is mean intensities with SD (quantified > 10 cells
666 from each set, n = 3). D) oAβ (1 μM) induced membrane damage in undifferentiated SH-SY5Y
667 cells, detected as uptake of the membrane-impermeable dye propidium iodide (PI) in presence
668 of 5 mM EGTA in PBS. Significant enhancement of PI uptake within 30 min of oAβ treatment
669 was observed in confocal images and quantified by flowcytometry (n = 6). E) Enhanced Lamp1
670 surface staining was detected in undifferentiated SH-SY5Y cells within 30 min of exposure of
671 oAβ (1 μM), as an indicator of lysosomal membrane fusion with the plasma membrane as
672 mechanism of membrane repair process. F) Lamp1 surface staining was quantified from
673 intensity (plotted mean ± SD) measurements by defined ROI in the image J. (number of cells
674 n for; control = 51, Aβ_15 min = 42 and Aβ_30 min = 6). Mann-Whitney t-test was performed

675 to validate the significance. G) Undifferentiated SH-SY5Y cells incubated with extracellularly
676 applied oAβ (1 μM) internalize to early-endosomes (Rab 5) and lysosomes (Lamp1) in
677 substantial quantity within 30 min. Here, the images are after 1.5 h of incubation. H) The
678 transferred non-degradable oAβ-TMR (red) end up to lysosomes (Lamp 1, green) of acceptor
679 cells in the co-cultured cells. However, gradual accumulation and formation of extra-large
680 lysosomes was observed about 48 h. Scale bars are10 μm.
681
682
683 **Figure 5.** Schematic summary to show the involvement of oAβ induced membrane damage
684 and membrane repair process in direct cell-to-cell transfer of oligomers via TNTs. Exocytosis
685 is followed by fusion of lysosomal membrane to reseal the damaged membrane on the outer
686 leaflet of the plasma membrane. Then, the repair process is finalized by endocytosis to re-
687 establish the plasma membrane.
688
689
690
691
692
693
694
695
696
697
698
699
700
701
702
703
704
705
706
707

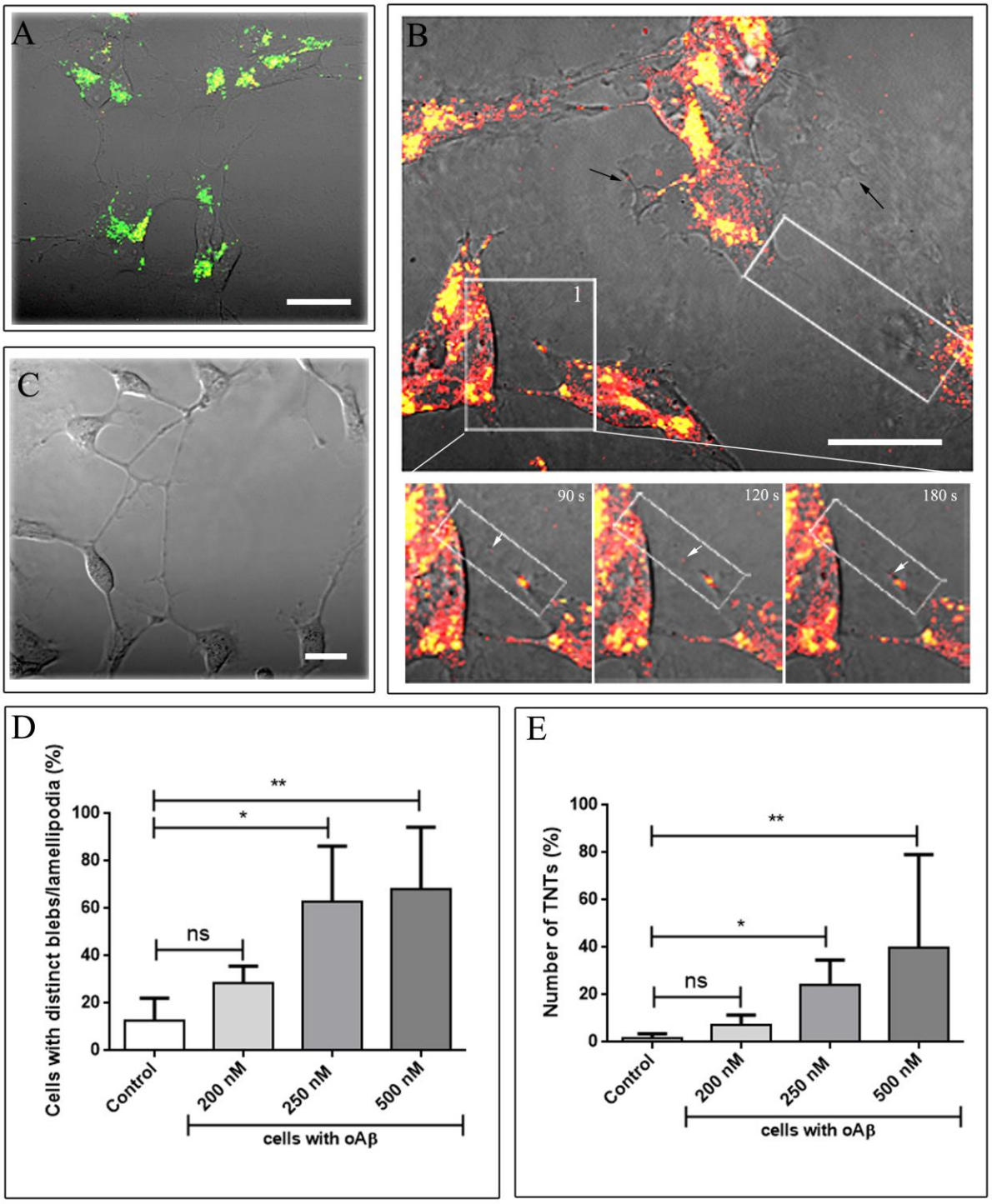

Figure 1

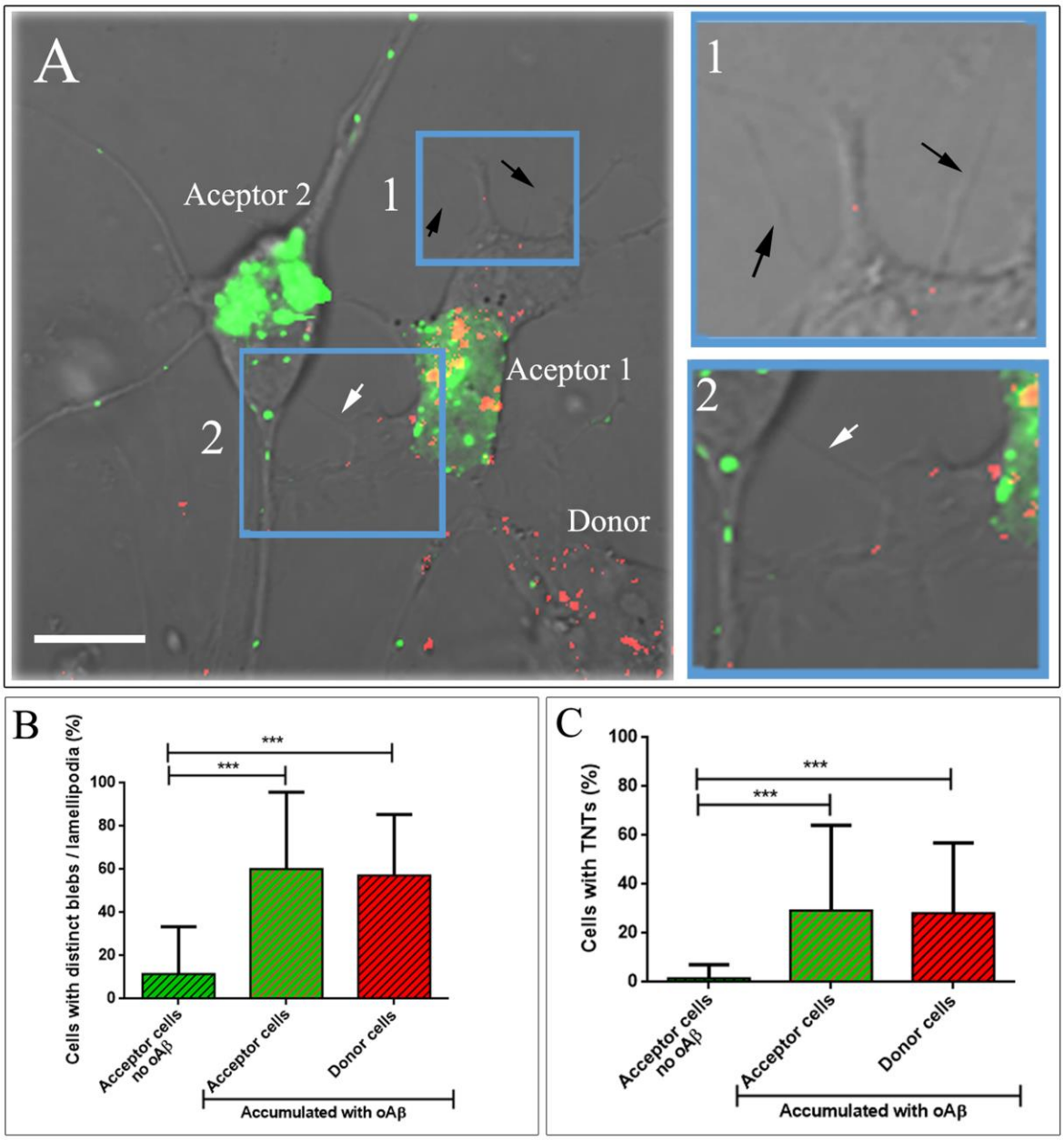

Figure 2

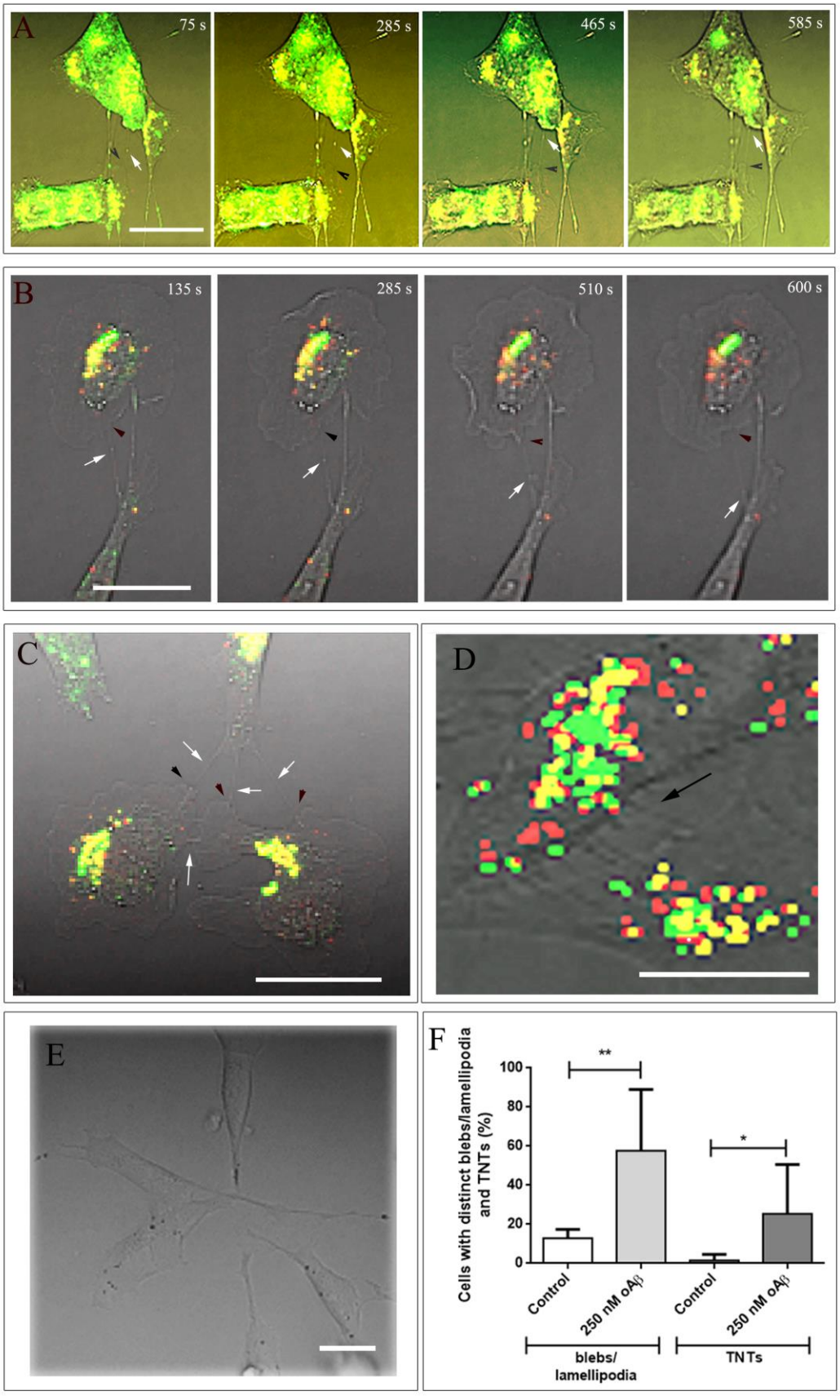

Figure 3

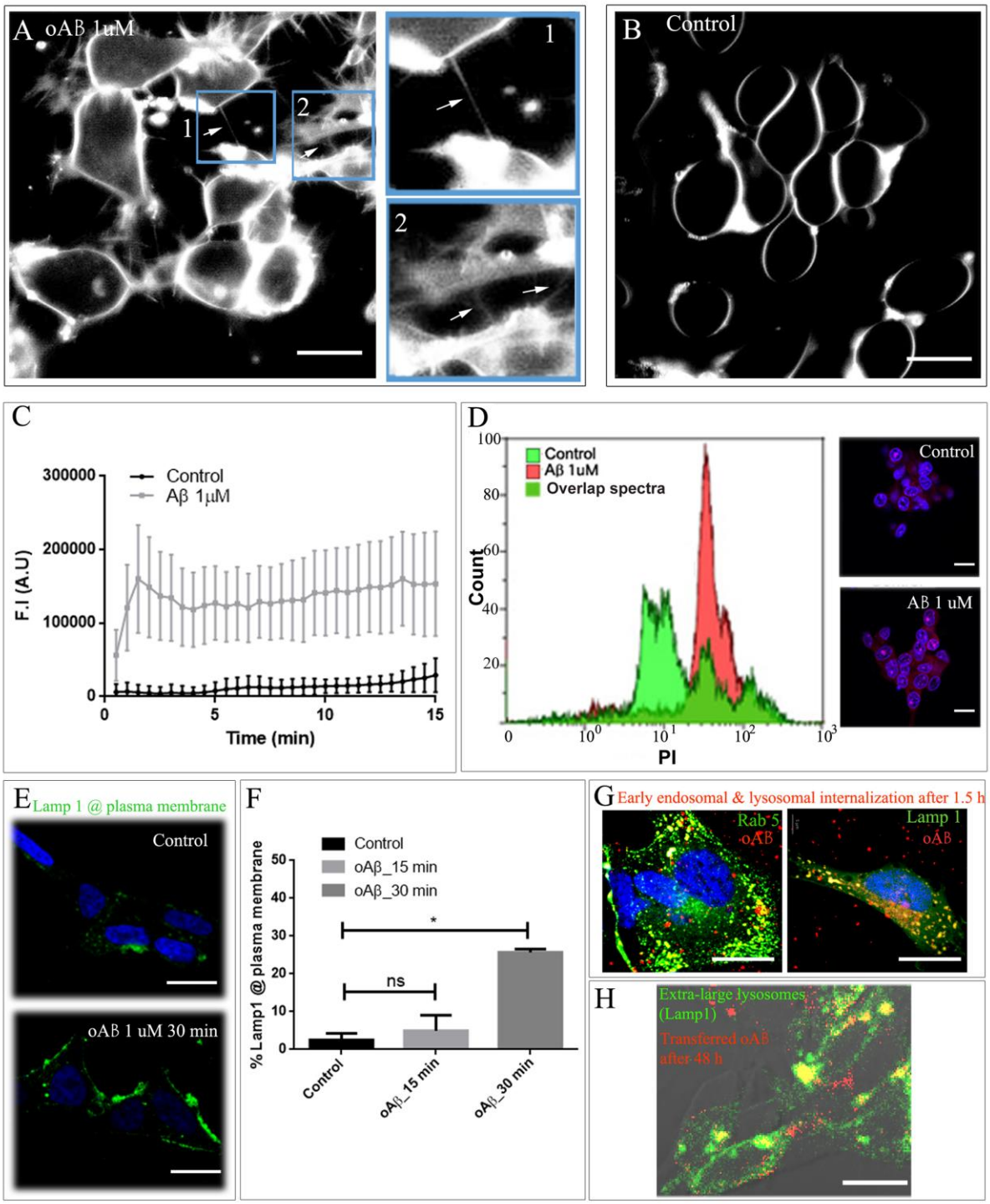

Figure 4

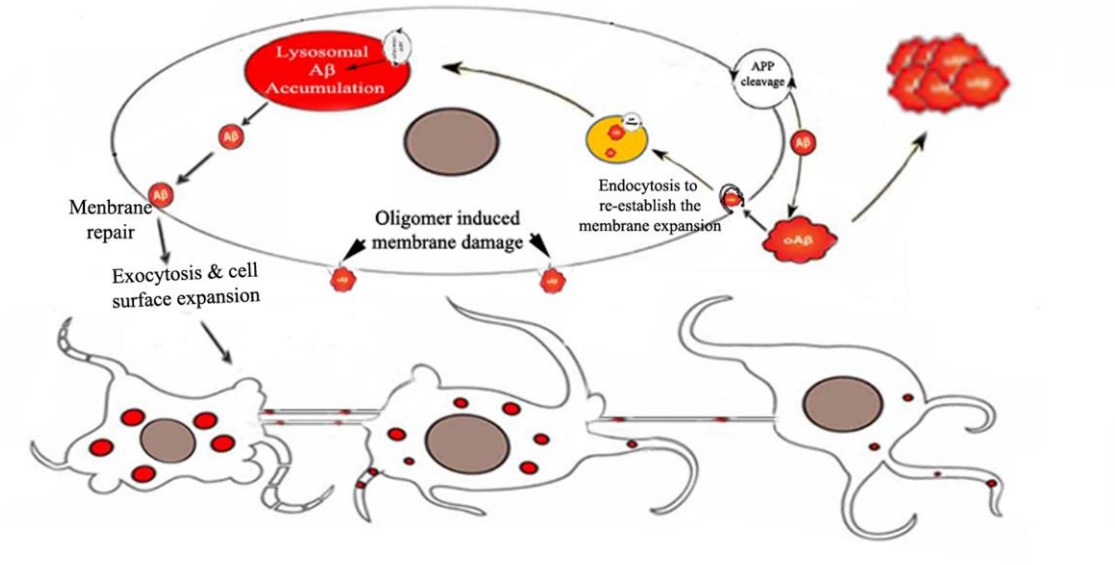

Figure 5